NORTH SEA FLOW MEASUREMENT WORKSHOP
measuring for the energy transition

Meeting the Challenges of CO_2 Measurement with a new kind of Orifice Meter

Phil Stockton, Accord Energy Solutions Ltd
Allan Wilson, Accord Energy Solutions Ltd
Richard Steven, DP Diagnostics

1 INTRODUCTION

The flow measurement of Carbon Dioxide (CO_2) rich streams, such has high CO_2 concentration natural gas and CO_2 mixes and Carbon Capture and Storage (CCS) processes, presents a number of potential challenges. One of these challenges concerns the physical properties of CO_2. For example, its compressibility exhibits significant non-ideal behaviour, notably at pressures and temperatures likely to be encountered in CCS processes. Additionally, through a process called 'molecular thermal relaxation' the molecular structure of CO_2 has the ability to attenuate ultrasonic meter acoustic signals. Furthermore, CO_2 can undergo phase changes through the CCS processes ranging from single phase gas, liquid, dense phase to two-phase.

Though the properties of CO_2 can be reliably predicted by several equations of state, the common presence of impurities, (N_2, H_2, CH_4, etc) can have a significant impact on these properties and therefore compromise uncertainty in the field.

In 2020, Kocbach et al [1] provided a review of the main available options for CO_2 measurement for CCS. They considered four meter types: Coriolis, ultrasonic, Venturi and turbine meters. This paper proposes a fifth alternative that has been in development over the past year: a new and improved methodology for operating and calculating flow through an orifice meter.

The authors have presented two previous papers, at the 2019 and 2020 NSFMWs, in which advantage is taken of the orifice meter's three differential pressure readings from the diagnostic system 'Prognosis': primary (ΔP_t), recovered (ΔP_r), and permanent pressure loss (ΔP_{PPL}) to reduce the uncertainty in the measured flow rate through an orifice meter. In these papers each of the differential pressure measurements was used independently to calculate flow rate, and each had its own flow coefficient, denoted C_d, K_r, and K_{ppl}, respectively. The 2019 paper introduced techniques from data reconciliation to reduce uncertainty. This was extended in 2020 to take advantage of temporal redundancy in the data using a Kalman filter to further reduce uncertainty. These techniques were collectively described under the term: 'Maximum Likelihood Uncertainty' (MLU).

A radically different approach is now presented. All three DPs are used to develop a new equation to calculate flow rate from first principles. It utilises momentum balances in the upstream and downstream sections of the orifice meter and a Bernoulli energy equation in the upstream section.

This new flow equation is significantly different in form to the ISO 5167-2 [2] flow equation. The ISO 5617-2 discharge coefficient compensates for the use of the known orifice meter beta rather than the theoretically required but unknown ratio of vena contracta to meter diameter. However, this new equation introduces a velocity head loss coefficient to account for mechanical losses while explicitly calculating the vena contracta diameter.

With no alteration to the primary orifice meter system the ISO 5167-2 flowrate calculation is still unaffected and available. This new equation is not presented as

an alternative to the traditional method but a supplemental aid to further improve the orifice meter's performance.

Incorporating the new and traditional equations into the mass balance constraints in the MLU calculations can significantly reduce the system's overall flowrate prediction uncertainty, while increasing the metering system's flow turn-down.

The equations and method have been developed for both incompressible and compressible flow. The compressible equations have the added benefit that the expansibility factor can be calculated in two ways: first according to ISO 5167:2 and second, assuming a reversible expansion from a calculated upstream pressure and vena contracta. This redundancy also allows the value and uncertainty of the isentropic coefficient of the gas to be improved in-situ, in accordance with the data. The efficacy of the method has been tested and demonstrated using real data obtained from the calibration of orifice meters with three pressure taps.

This new approach is presented as a development of, and complementary to, the well-established standard single DP flow equation, but one that also incorporates and exploits the additional information that three DP measurements generate. The above developments render the new approach, termed Oculus, appropriate for any flow measurement application, inclusive of CO_2.

The application of the MLU and Kalman Filter equations, and algorithms, that comprise the Oculus method, combine the multiple instrumentation readings, equipment settings, associated uncertainties, and governing physical laws, to reconcile measurements such that the whole makes physical sense. The technique can improve best estimates of not just measured system variables but even unmeasured variables. This includes values of the physical properties of the fluid. This feature is exploited to improve the estimate of the isentropic exponent in the examples presented in this paper. It is anticipated that this can also be extended to the density and Joule Thomson coefficient. Hence, this makes the Oculus orifice flow meter a good candidate to measure the flow of gases whose physical properties are difficult to determine or are sensitive to flowing conditions such as CO_2.

2 A NEW ORIFICE FLOW RATE EQUATION - INCOMPRESSIBLE

2.1 Traditional Orifice Flow Rate Equation

The flow of a fluid through an orifice plate installed in a pipe is illustrated schematically in Figure 1:

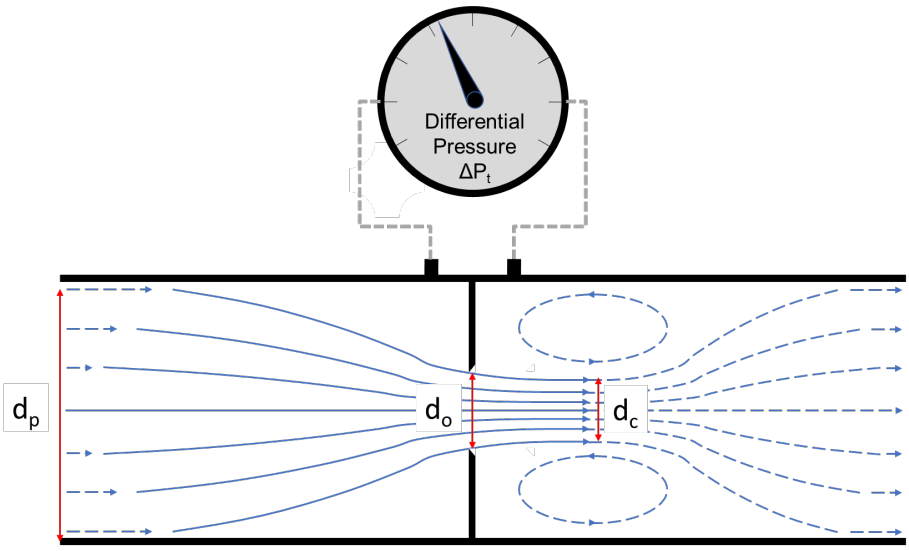

Figure 1 - Schematic of Orifice Plate Flow Measurement

The flow is derived from the differential pressure measurement across the plate ΔP_t, a knowledge of the orifice (d_o) and pipe (d_p) diameters, the fluid density (ρ) and a discharge coefficient (C_d) that can be determined from a correlation such as that presented in in ISO 5167-2 [2]. The equation for incompressible mass flow is:

$$Q_m = \frac{C_d \pi d_o^2 \sqrt{2\rho \Delta P_t}}{4\sqrt{(1-\beta^4)}} \quad (1)$$

Where:

Q_m Mass flow rate (kg/s)

β Ratio of orifice to pipe diameter (d_o/d_p)

Equation (1) is derived from Bernoulli's equation and the conservation of mass. It has the same form to that for a Venturi meter in which the C_d term has a value close to 1.0 and which accounts for minor mechanical (frictional) losses and departures from ideality. However, in the case of the orifice meter the C_d term is typically around a value of 0.6. This is because C_d for the orifice is accounting for two principal effects:

- Mechanical losses (similar to the Venturi);
- The contraction of the fluid jet downstream of the orifice.

The fluid jet continues to converge downstream of the orifice to a point of minimum diameter (d_c) called the vena contracta (as indicated in Figure 1). Since d_c is not known, (and which varies with the flowing conditions), the orifice diameter is used in its place and the change in flow prediction caused by this replacement is corrected for by C_d. This adjustment is significantly greater than that due to the mechanical losses.

At first sight, it might be anticipated that, in contrast to the smoothly contoured venturi, the sharp edge orifice might cause significant eddying and frictional effects upstream of the plate. Measurements of the pressures and velocities throughout the flow field upstream and downstream of the plate using a 3-D laser Doppler anemometer system have been made by Morrison et al [3]. Diagrams from the paper illustrating the velocity vector field are reproduced below in Figure 2:

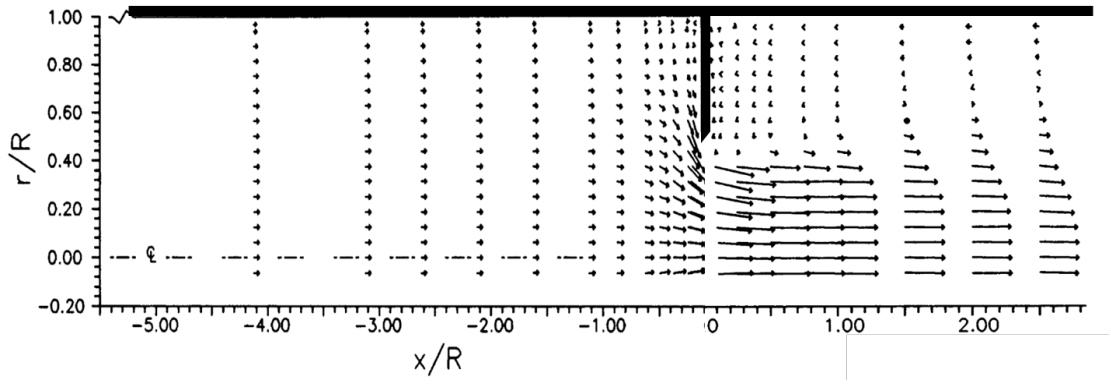

Figure 2 - Orifice Plate Vector Field

The arrows in the figure indicate the direction of flow and their length indicates the magnitude of the velocity associated with the fluid at that point. The figure illustrates the smoothly contoured streamlines upstream of the orifice indicating little induced turbulence[1] and hence small mechanical losses (there is a small zone of recirculation at the upstream base of the orifice). Though the orifice does not have a converging pipe section to the orifice aperture, the fluid forms its own smoothly converging jet. Hence, rather counter-intuitively, flow into the orifice and Venturi meters form remarkably similar stream tubes.

In contrast, downstream of the orifice there are large zones of recirculation surrounding the fluid jet, in which more significant induced turbulence and hence

[1] Induced turbulence is that caused by the flow passage shape in excess of that normally present in the flow. The energy resident in the turbulence is not usually recovered as mechanical energy and is consequently converted to heat – see [3].

losses are experienced. Downstream of the orifice is where the mechanical losses occur; the absence of a smooth divergent pipe section results in considerable induced turbulence.

If the vena contracta diameter could be determined, then the element of the discharge coefficient that compensates for the use of d_o in place of d_c could be eliminated and the discharge coefficient, compensating for losses alone, would be much closer to one, similar to the venturi.

The introduction of third pressure tapping provides additional measurements that can be used to calculate the vena contracta diameter and generate a new flow rate equation for the orifice meter.

2.2 New Orifice Flow Rate Equation – Incompressible Flow

The orifice plate with three pressure tappings and three differential pressure measurements is illustrated schematically in Figure 3:

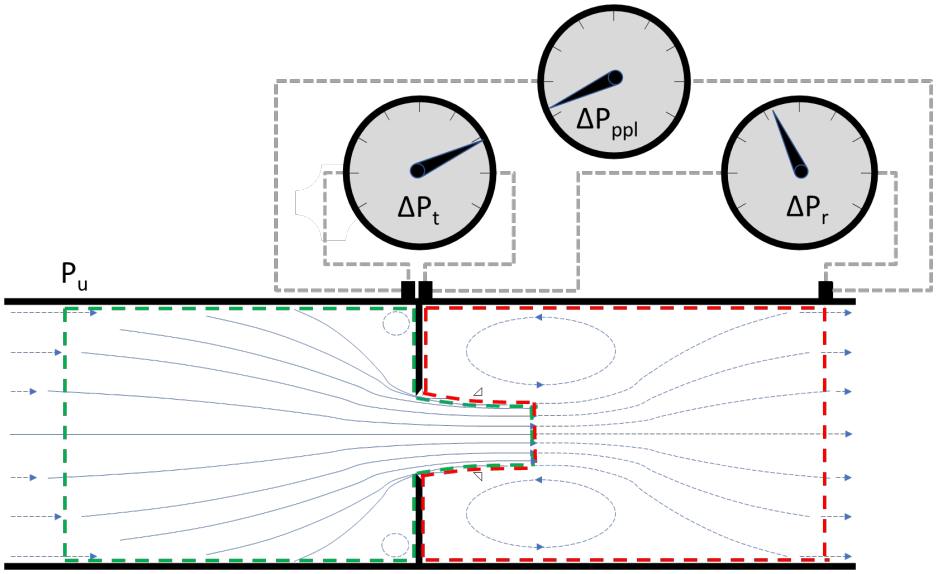

Figure 3 - Schematic of Orifice Plate with Three Differential Pressure Measurements

In addition to the differential pressure measurement across the orifice plate ΔP_t, the introduction of the third downstream pressure tapping allows the measurement of the recovered pressure ΔP_r and pressure loss ΔP_{ppl} differentials to be measured.

Also indicated in the Figure 3 are the outlines of two control surfaces:

- The upstream control surface, outlined in green, extends from a plane, perpendicular to the axial fluid flow, (where the normal pipe flow is just unaffected by the orifice), along the pipe walls, across the orifice plate upstream surface, through the orifice aperture, over the surface of the fluid jet protruding into the downstream section and finally covering the vena contracta surface normal to the flow.
- The downstream control surface, outlined in red, extends from the vena contracta and fluid jet surface across the downstream side of the orifice plate along the pipe walls to a plane where the normal pipe flow is resumed.

The pressure downstream of the orifice at the vena contracta is assumed to be the same as that just outside the streamlines of the jet and on the back side of the orifice plate. Hence, the measured pressure at the pipe wall, (downstream corner tapping), is assumed to be the same as vena contracta pressure. Urner [10] applies this same assumption in the development of Equation (7) for the Pressure loss in ISO 5167-2 [2].

The analysis is based on measuring the differential pressure across the orifice at the plate faces, i.e., using corner tappings. In practice, most tappings are flange mounted and located away from the face. The desired corner tapping differential pressure is calculated from a flange-based measurement using the components of the ISO 5167-2 discharge coefficient and is discussed further in Appendix A.4.

Three sets of physical laws can be applied across these control surfaces:

- Conservation of mass flow
- Conservation of momentum
- Conservation of energy.

From the application of the relevant equations over the control surfaces, a new equation for the mass flow has been derived:

$$Q_m = \frac{\pi d_o^2}{4\beta^2} \frac{\Delta P_r \sqrt{\rho}}{\sqrt{2(1-\beta^2)\left(\Delta P_r + \Delta P_{ppl}\right)}} \tag{2}$$

The full derivation of this equation is presented in Appendix A.

The form of the equation is fundamentally different to the traditional flow equation (1) and not a slight adjustment to it. This is advantageous for the application of the Oculus method as the more independent the methods of estimating flow are, the lower the resulting uncertainty in the reconciled quantities.

As part of the development of this equation, the vena contracta diameter and the unmeasured pressure (P_u) on entry to the upstream control surface are implicitly determined. (Appropriate rearrangement of the equations presented in Appendix A allow these quantities to be calculated explicitly).

In the form presented above in (2), the new equation does not have a discharge coefficient. This is an ideal version of the new equation as there are mechanical losses which are accounted for in an expanded version described below. However, it is interesting to observe how well this ideal equation predicts flow rates in comparison with the standard equation.

This was tested using real data from a calibration facility in which water flows through an 8", 0.4 beta orifice meter with three differential pressure measurements. Measured input variables, relative uncertainties and absolute uncertainties are listed in Table 1, which also includes the reference meter flow $Q_{m,ref}$.

The flow rate calculated using equation (2) is:

- Ideal New Equation: 42.879 kg/s

The new equation, without accounting for losses, is 3.5% below the reference value. In comparison, without the application of the discharge coefficient the traditional flow equation would be 40% low. The new equation is much closer because it implicitly calculates the vena contracta diameter:

Table 1 - 8", 0.4 Beta Orifice DP Meter Variables and Parameters

Measurement	Unit	Value	Relative Uncertainty
ΔP_t	Pa	100,448	±0.4% of max
ΔP_r	Pa	17,303	±0.4% of max
ΔP_{PPL}	Pa	83,169	±0.4% of max
d_p	m	0.2026	±0.4%
d_o	m	0.0810	±0.1%
ρ	kg/m^3	998.2	±0.27%
C_d	-	0.6019	±0.50%
$Q_{m,ref}$	kg/s	44.444	±0.15%

- Vena contracta: 0.0639 m

This serves to illustrate that the upstream mechanical losses are relatively minor and that the main component of C_d is accounting for the use of the orifice diameter in place of the vena contracta diameter.

Mechanical losses can be included in the equations by adding a loss term to the Bernoulli equation associated with the upstream control surface. This has been expressed as a number, N_{luc}, of dynamic pressure terms, expressed in the form:

$$L_{uc} = \frac{N_{Luc}\rho U_p^2}{2} \tag{3}$$

Where,

L_{uc} Losses term from upstream pressure to vena contracta (kg/ms^2)

U_p Pipe velocity (m/s)

This is distinct to a discharge coefficient as it is related to the approach taken when calculating pipe losses in terms of velocity heads [4]. When accounting for losses the new equation becomes:

$$Q_m = \rho \frac{\pi d_o^2}{4\beta^2} \sqrt{\frac{(1-\beta^2)(\Delta P_r + \Delta P_{ppl}) - \sqrt{\left((1-\beta^2)(\Delta P_r + \Delta P_{ppl})\right)^2 - N_{luc}\Delta P_r^2}}{\rho N_{luc}}} \tag{4}$$

The inclusion of the losses term is described fully in Appendix A. At first sight, the mass flow appears to be inversely proportional to the square root of N_{luc} and therefore increase asymptotically to infinity as N_{luc} tends to zero. However, it also appears in the numerator and actually tends to the ideal version of the equation as N_{luc} tends to zero.

A problem remains however, regarding the value of N_{luc} which is an empirical constant and therefore needs to be determined experimentally.

The development of the Reader-Harris Gallagher equation for the discharge coefficient C_d, presented in ISO-5167 [2], is described extensively [5]. The equation was fitted to data collected from numerous sources over a considerable number of years. Hence, encoded in the Reader-Harris Gallagher equation is a wealth of experimental data. This implicit data was accessed by equating equations (1) and (4) to generate the following for the determination of N_{luc}:

$$N_{luc} = (1-\beta^4)^2 \left(\frac{1}{C_d^2(1+\beta^2)\beta^4} - \frac{\Delta P_r^2}{4C_d^4\beta^8(\Delta P_r + \Delta P_{ppl})^2} \right) \tag{5}$$

For the example described above in Table 1:

- N_{luc}: 6.378
- Mass Flow Rate: 44.517 kg/s

The new equation, after accounting for losses, is 0.16% above the reference value. This may be compared with the traditional equation (1) which predicts:

- Traditional Flow Rate: 44.523 kg/s

Which is 0.18% above the reference value.

Though C_d does appear in the new flow rate equation via the losses term, its impact on the mass flow rate is considerably reduced compared with its direct impact in the traditional flow equation.

This analysis is extended over the full range of the data points obtained from the test in Section 2.5.

The uncertainty in the new equation has been calculated according to the methods described in the Guide to Expression of Uncertainty in Measurement (GUM) [6] and compared with that for the traditional equation (ISO 5167 [2]):

- New equation: ±1.39%
- Traditional equation: ±0.59%

The new equation does not provide an improved uncertainty in the calculated flow rate compared with the traditional approach. However, it does provide a relatively independent estimate of flow that still exhibits a reasonably low uncertainty.

The new equation is not intended as a replacement of the current equation, which is well established, named in contracts, and has worked extremely well over many years. It is complementary and was developed as an independent approach based on fundamental physics. It is possible its uncertainty could be reduced if the estimates of N_{luc} could be improved but the real advantage of the new equation is its inclusion in the data reconciliation and Kalman filtering techniques i.e., the Oculus approach, described in previous papers by the authors [7] and [8] and discussed in the next two sections.

2.3 Application of Maximum Likelihood Uncertainty

At the 2019 NSFMW, the authors presented: 'Data Reconciliation In Microcosm - Reducing DP Meter Uncertainty' [7]. Mathematical techniques, based on steady state data reconciliation, were developed to improve the performance of flow meters, including fine adjustments to the stated flowrate prediction while lowering uncertainty. These techniques were collectively described under the term: 'Maximum Likelihood Uncertainty' (MLU).

MLU requires multiple instrument readings. In the case of differential pressure (DP) meters this is provided by axial pressure profile analysis facilitated by the third pressure tapping generating the three differential pressure readings: primary DP (ΔP_t), recovered DP (ΔP_r), and permanent pressure loss (ΔP_{ppl}). Each of these differential pressures was used independently to calculate the flow rate and each of these flow calculations has its own flow coefficient, denoted C_d, K_r and K_{ppl}, respectively. These flow rate equations were all of a similar form:

$$Q_{m,t} \propto C_d\sqrt{\Delta P_t} \tag{6}$$

$$Q_{m,r} \propto K_r\sqrt{\Delta P_r} \tag{7}$$

$$Q_{m,ppl} \propto K_{ppl}\sqrt{\Delta P_{ppl}} \tag{8}$$

MLU, applied to DP meters, reconciles the three measured DPs so that the three resultant calculated flow rates equal one another (satisfying mass balances) and the recovered and PPL DPs sum to the primary DP (satisfying the DP balance). It does this in a statistically optimal fashion in accordance with the uncertainties in the measurement sensors and associated input parameters.

Instead of using equations (7) and (8), equation (4) was used in the MLU algorithm as input to the mass balance along with the traditional equation (1). The same DP balances were retained. Note that it is possible also to include equations (7) and (8), but for the purposes of this analysis they were excluded so the impact of the new equation could be determined more explicitly.

Application of the Kalman Filter

The 2019 paper applied data reconciliation techniques to a single set of flow meter measurements obtained simultaneously at a specific time. In effect this is 'steady state MLU'. The technique was extended in the 2020 paper [8] to take advantage of time, that is, the method was extended from a static to dynamic data analysis.

In essence, steady state MLU extracts the maximum information from the existing measurements in order to obtain optimal estimates of the system variables at one instant in time. Time provides an extra dimension in which repeated measurements by the same instruments generate additional information that can be exploited by the MLU techniques to improve the estimates of flow rate and further reduce its uncertainty.

For example, for the case of the DP meter with three flow equations using three flow coefficients, it was assumed that flow coefficients remained ostensibly constant in time. This extra information was incorporated into the MLU technique using the Kalman Filter. Kalman Filters are typically used to model dynamic systems where some relationship defines the evolution of the system state with time and updates the state with measurements. By analyzing multiple data grabs at different times, the Kalman Filter reduces the flow rate uncertainty and improves the estimation of the flow coefficients, thereby self-tuning the DP meter in-situ.

The new equation was incorporated into the Kalman filter approach also. The values of N_{luc} and C_d were treated as independent variables and their estimated values were thereby improved. In an enhancement to the method presented in 2020 [8] C_d was expressed as a function of Reynolds number and the parameters of this function were assumed to be constant through time. The value of N_{luc} was afforded some variation with flow by the introduction of process noise which is a feature of the Kalman filter. The process noise represents the uncertainty in the physical model. Though the initial assignment of this process noise is a matter of judgement, it is an adjustable parameter and its correct value is ensured using statistics output by the Kalman filter[2].

The flow coefficients were focussed on in the previous analysis, but the Kalman filter also improved the estimates of all the parameters in the equations, which included, for example, the orifice expansibility coefficient and the isentropic exponent. Indeed, this applies to any of the measured or unmeasured variables.

This feature is particularly advantageous for the measurement of CO_2 which presents challenges in terms of physical properties which exhibit non-ideal behaviour, notably at pressures and temperatures likely to be encountered in CCS processes. The auto-tuning of the physical properties to be consistent with the mass, momentum and energy conservation constraints will mitigate the impact of uncertainties encountered in the field, for example the presence of impurities, rapidly changing compressibility, incipient liquid condensation near the two phase region, etc.

It should be noted that the MLU approach also performs this improvement in the parameters of the system, but the Kalman filter enhances this feature by utilising their behaviour as a function of time.

2.4 Tests with Water Data

The data from the calibration facility for water flow through an 8", 0.4 beta orifice meter described above in Table 1 was used to assess the various approaches over a number of data points from the test. The results presented in Figure 4 compare the difference in flow rate with the Coriolis water reference meter for the standard equation (blue circles) and new equation (orange squares) at each data point.

[2] These are the innovation and auto-correlation statistics generated by the Kalman Filter.

The figures along the x-axis indicate the reference mass flow rate associated with the data points. Note that this is not a scatter plot. Each pair of points allows a direct comparison the two equations at the reference flow and are ordered sequentially (ordinally) from left to right in terms of increasing flow.

Incompressible water flow metering is simpler than compressible gas flow metering, and as such water flow meters have relatively low mass flow prediction flowrate uncertainties. Hence, with the reference and standard water flow orifice meters having low flowrate prediction uncertainties the effect of the new method is modest. The effect of this method is more pronounced with compressible gas flow metering.

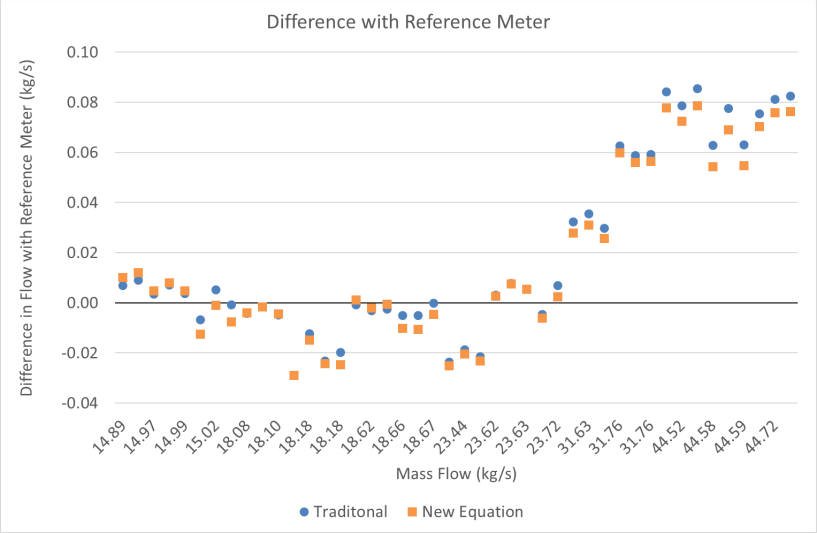

Figure 4 – 8" 0.4 Beta Orifice Mass Flow Rate Difference with Reference Meter Traditional and New Equations

As can be observed the new equation predicts similar flow rates to the traditional equation, though it is marginally closer to the reference meter at higher flow rates.

The data from the test is not ideal with regard to the application of the Kalman filter. The test points were obtained at intervals with step changes in the flow occurring between points. The Kalman Filter still works but the maximum information cannot be extracted from the full time series data. This means that the potential uncertainty reduction offered by the Kalman filter cannot be exploited.

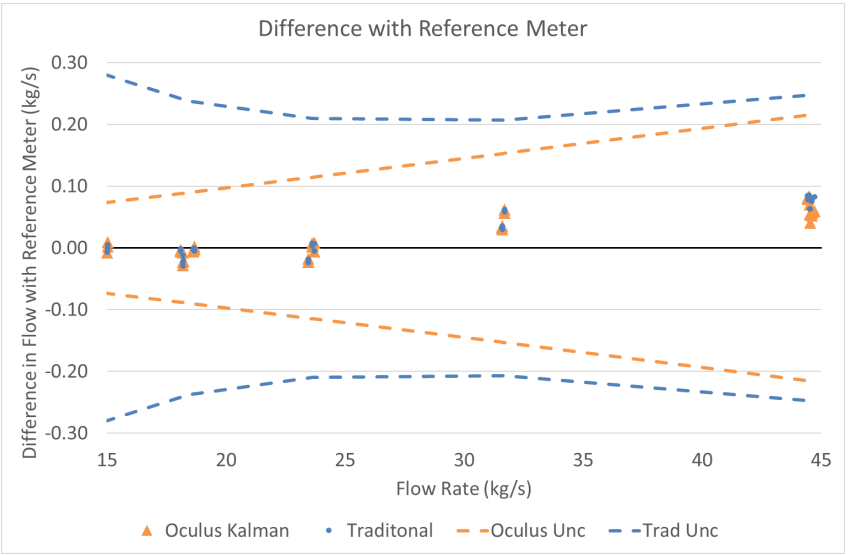

Figure 5 – 8" 0.4 Beta Orifice Mass Flow Rate Difference with Reference Meter Traditional and Oculus Kalman MLU Including Uncertainties

Figure 5 presents the results of the Oculus Kalman filter approach, which is in terms of a scatter plot. The Kalman Oculus results closely follow the traditional values except for the final data points at the highest flow rates where the agreement with the reference meter improves.

Also shown on the plot are the 95% uncertainty confidence limits for the Kalman Oculus and traditional values. The reduction in uncertainty delivered by the Oculus approach is evident especially at lower flow rates. This means that Oculus effectively extends the working range of the orifice meter.

With these four reported flows based on different measurement methods:

- a reference meter;
- the traditional mass flow is based on the differential pressure across the orifice plate;
- the new equation is based on the recovered and permanent pressure loss differentials;
- the Oculus results are based on a combination of all three differential pressure measurements;

there is good agreement between them and all are well within the standard reported uncertainty.

It does appear that the uncertainty in any one of the reported flow rates is lower than the standard uncertainties calculated using the Type B approach as described in the GUM [6]. Indeed, the uncertainties generated by Oculus could be considered to eb Type A uncertainties, that is: "method of evaluation of uncertainty by the statistical analysis of a series of observations". By extension this also means that in effect the additional measurements allow the uncertainty in the traditional reported mass flow to be reduced. In particular, the de facto uncertainty of ±0.5% (quoted in [2]) for the discharge coefficient C_d may potentially be a candidate for reduction as this covers a wide range of operation. Though not the subject of this paper, a more detailed analysis which allows a reduction in the standard flow rate uncertainty is a possibility. This would allow the flow calculated according to ISO 5167-2 [2] to be reported with a reduced uncertainty in accordance with a Type A uncertainty as discussed in the GUM [6].

Oculus has been shown to be applicable to orifice meters with incompressible flows. However, such incompressible flows, i.e., liquid flows, are known to be meter-able by various technologies at very low flowrate prediction uncertainties. Hence, traditional orifice meters in water flow service give rather low flowrate prediction uncertainties. Therefore, Oculus only has the opportunity to make marginal further improvements. This is what is seen in this example. The traditional orifice meter never deviates from the reference meter by more than 0.2%. Hence, for this application Oculus can only offer small improvements in mass flow prediction and associated uncertainty. It is with compressible flow, i.e., gas flow, where Oculus can make a more substantial impact. That is now discussed.

3 A NEW ORIFICE FLOW RATE EQUATION - COMPRESSIBLE

3.1 Traditional Orifice Flow Rate Equation

The traditional equation is modified for compressible flow by the inclusion of an expansibility factor (ε):

$$Q_m = \frac{\varepsilon C_d \pi d_o^2 \sqrt{2\rho \Delta P_t}}{4\sqrt{(1-\beta^4)}} \tag{9}$$

ε is determined, according to ISO-5167-2 [2], by:

$$\varepsilon = 1 - (0.351 - 0.256\beta^4 - 0.93\beta^8)\left(1 - \left(\frac{P_u}{P_c}\right)^{1/k}\right) \quad (10)$$

Where,

P_u Upstream pressure in main pipe flow just prior to influence of orifice (Pa)

P_c Downstream pressure at vena contracta (Pa)

k Isentropic exponent.

3.2 New Orifice Flow Rate Equation – Compressible Flow

For compressible flow, the incompressible versions of the Oculus equations can be utilised, and the result multiplied by the expansibility factor calculated according to equation (10).

However, the fact that the vena contracta diameter can be calculated using the new equation means that the expansibility can be calculated assuming a reversible expansion across the orifice jet to the vena contracta. This is similar to the approach adopted for Venturis.

Since the gas expansion can be accounted for in two different ways, this redundancy allows the value and uncertainty of the isentropic coefficient of the gas to be improved in-situ, in accordance with the data.

The development of the new orifice equation for compressible flow is a modification of that for incompressible flow. The same analysis over the upstream and downstream control surfaces is used along with the three sets of physical laws across these control surfaces:

- Conservation of mass flow
- Conservation of momentum
- Conservation of energy.

The equations are modified to recognise the change in density of the gas between the upstream plane, the vena contracta and the downstream plane.

An isentropic expansion is assumed to occur between the upstream plane and the vena contracta. The change in density can be calculated using the pressure difference between two locations and the gas's isentropic exponent.

An irreversible, adiabatic, (i.e. Joule Thomson), expansion is assumed to occur across the orifice between the upstream and downstream planes. The Joule Thomson coefficient of the gas can be used to calculate the change in temperature between the two planes, and along with the drop in pressure, the change in gas density obtained.

The MLU and Kalman filter techniques can then be applied using these equations for compressible flow. Additional parameters are now involved in the reconciliation, such as the gas density and isentropic exponent.

The above approach is similar to that originally adopted by Buckingham [9], though it has been extended to include the third pressure tapping and the Joule Thomson expansion.

3.3 Tests with CO_2 and Natural Gas Mixtures

Data from a calibration facility was obtained that compared the measurement results from an orifice meter (see Figure 7), against a reference turbine meter (see Figure 6) for natural gas with various concentrations of CO_2, ranging from 2% to 40% (molar). The orifice meter had a downstream pressure tap and the three DP transmitters required for the axial pressure profile diagnostic system Prognosis and the Data Validation system Oculus.

Figure 6 – 8" Turbine Meter

Figure 7 – 8" 0.564β Orifice Meter

The orifice meter diagnostic system Prognosis shows that the orifice meter system is operating correctly. Figure 8 reproduces the Prognosis results for a sample of the 49 bar data at varying carbon dioxide concentrations. All results inside the box indicates a correctly operating metering system.

The results presented in Figure 9 compare the percentage difference in flow rate with the reference turbine meter for the standard orifice meter and for when the orifice meter runs Oculus for natural gas containing 2% CO_2, i.e., a low concentration. There are four mass flowrates ranging from just over 1 kg/s to almost 4.5 kg/s.

As can be seen, for all four data points, Oculus reduces the difference with the reference meter flow in comparison with the traditional orifice measurement.

Figure 10 is a similar plot but with 40% (molar) CO_2 content, i.e., a high concentration:

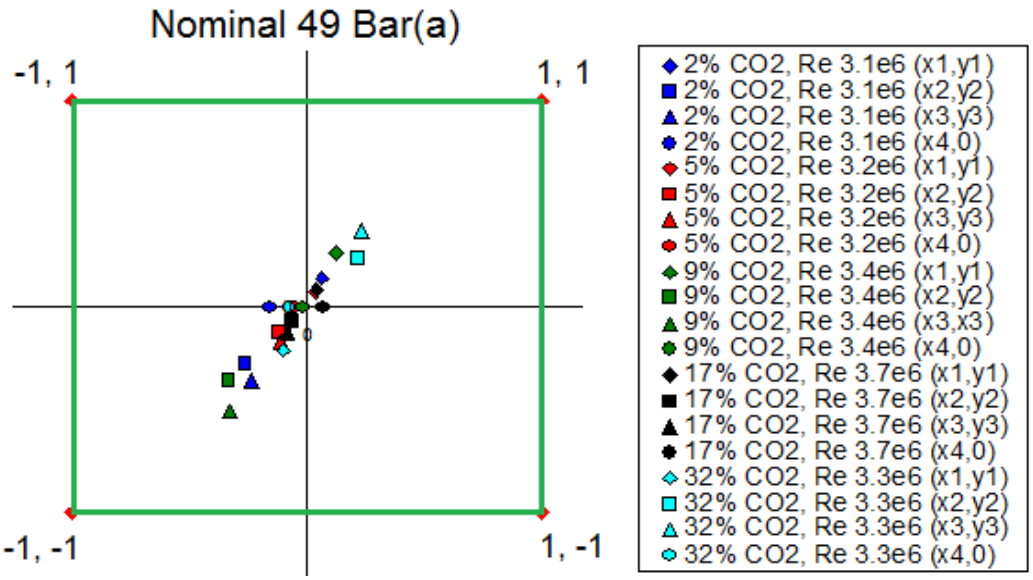

Figure 8 – Sample 49 Bar(a) 8", 0.564β Orifice Meter Prognosis Results for Varying CO_2 Concentrations

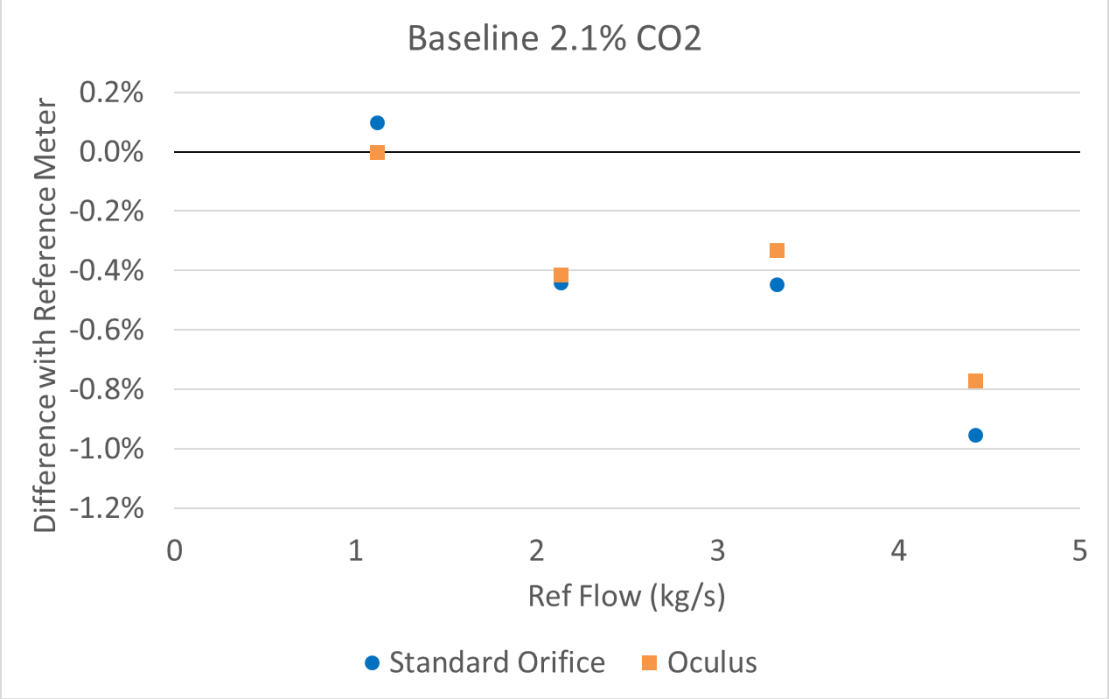

Figure 9 - Mass Flow Rate Difference with Reference Meter, Natural Gas containing 2% (molar) CO_2

Oculus improves the traditional orifice result and is significantly closer to the reference meter at higher flows.

There are 35 data points available and the mean absolute deviation for all the data points is presented in Table 2:

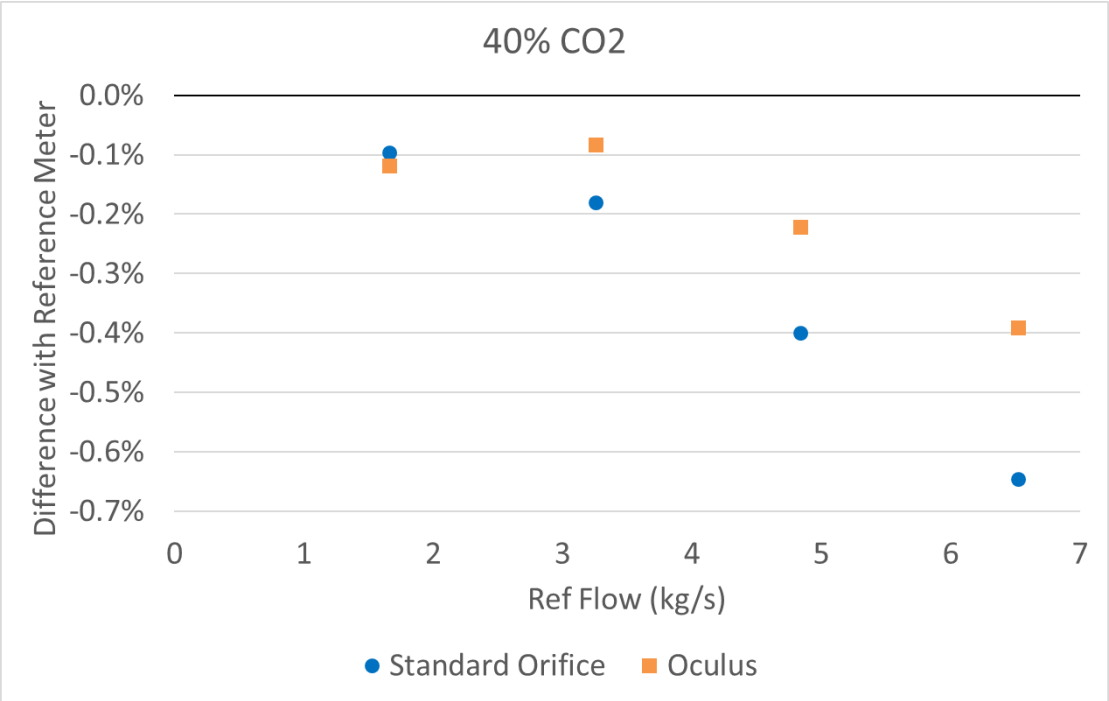

Figure 10 - Mass Flow Rate Difference with Reference Meter, Natural Gas containing 40% (molar) CO_2

Table 2 – Mean Absolute Deviation from Turbine Reference Meter, Natural Gas with Various CO_2 Concentrations

Meter Type	Mean Absolute Deviation (%)
8" 0.56 Beta Orifice Traditional	0.67%
8" 0.56 Beta Orifice with Oculus	0.51%

The orifice plate equipped with Oculus exhibits the lowest mean absolute difference across all the data points. The orifice meter with Oculus is shown to cope with high concentrations of carbon dioxide (≤40%) while giving a flowrate prediction uncertainty of approximately 0.5% at 95% confidence.

4 CONCLUSIONS

By taking advantage of the orifice meter's three differential pressure readings from the diagnostic system 'Prognosis', a new flowrate equation has been developed from first principles for the orifice plate. This has been used in conjunction with the standard ISO 5167-2 equation to provide an improved estimate of flowrate which exhibits a lower uncertainty than that associated with the standard equation. This has been achieved by employing the Oculus method which is based on MLU and Kalman filter techniques presented by the authors in two previous papers, at the 2019 and 2020 NSFMWs.

The efficacy of Oculus has been established for the incompressible case using water data from a calibration facility. However, for this application Oculus can only offer small improvements in mass flow prediction. It does improve the uncertainty (based on Type B input uncertainties) and extends the turndown of the meter.

It does appear that there is the potential for Oculus to improve the uncertainty in the standard reported flow rate. This can be achieved in situ, (i.e. as a live uncertainty), by considering the uncertainties quoted for Oculus as Type A according to the GUM [6], that is: "method of evaluation of uncertainty by the statistical analysis of a series of observations".

The equations have been extended to handle compressible gas flow, where Oculus can make a more substantial impact. This has been tested with CO_2 and natural gas mixtures obtained from a calibration facility. The orifice plate equipped with Oculus is shown to cope with high concentrations of carbon dioxide (≤40%) while consistently improving the agreement with the reference meter when compared to the results from the standard orifice meter.

This orifice meter equipped with Prognosis and Oculus is a viable meter capable of meeting the challenges of CO_2 and natural gas measurement whilst enjoying the following benefits:

- Lowest cost meter
- No calibration requirements
- Comprehensive diagnostic system available without calibration
- Ability to handle two phase flow
- Low mass flow uncertainty comparable with other meter types
- Improvement in the estimate of physical properties associated with the flowing fluid.

It is worth mentioning the future potential improvements of Oculus for measuring CO_2 flow. The values of the isentropic exponent and Joule Thomson coefficient have been improved by the Oculus approach in the analysis presented. However, it is proposed to extend the method to incorporate other properties: e.g. density calculations, compositional data, vapour liquid equilibria and phase transitions.

What the orifice plate loses in pressure drop it compensates for with information.

NOTATION

A_c	Area of vena contracta (m^2)
A_o	Area of orifice (m^2)
A_p	Area of pipe (m^2)
C_d	Discharge coefficient
C_{dn}	C_d Downstream flange term
C_s	C_d Reynolds number term
C_{up}	C_d Upstream flange term
C_∞	C_d at infinite Reynolds number
d_c	Vena contracta diameter (m)
d_o	Orifice diameter (m)
d_p	Pipe internal diameter (m)
K_{PPL}	Permanent pressure loss coefficient
K_r	Recovered pressure coefficient
L_{uc}	Losses from upstream to vena contracta (Pa)
N_{Luc}	Number of dynamic pressure terms for L_{uc} (Pa)
P_c	Pressure at vena contracta (Pa)
P_d	Pressure at downstream tapping (Pa)
P_o	Pressure in jet stream at orifice aperture (Pa)
P_{od}	Pressure downstream of orifice at wall (corner tapping) (Pa)
P_{ou}	Pressure upstream of orifice at wall (corner tapping) (Pa)
P_u	Pressure upstream (Pa)
P_1	Q_m Mass flow rate (kg/s)
$Q_{m,l}$	Mass flow rate from permanent pressure loss (kg/s)
$Q_{m,r}$	Mass flow rate from recovered pressure differential (kg/s)
$Q_{m,ref}$	Reference meter mass flow rate (kg/s)
$Q_{m,t}$	Mass flow rate from orifice pressure differential (kg/s)
U_c	Average velocity at vena contracta (m/s)
U_o	Average velocity at the orifice (m/s)
U_p	Average pipe velocity (m/s)
β	Ratio of the orifice diameter to pipe diameter
ΔP_{ppl}	Permanent pressure loss differential relative to upstream corner tapping (Pa)
$\Delta P_{ppl,fl}$	Permanent pressure loss differential relative to upstream flange tapping (Pa)
ΔP_r	Recovered pressure differential relative to upstream corner tapping (Pa)
$\Delta P_{r,fl}$	Recovered pressure differential differential relative to upstream flange tapping (Pa)
ΔP_t	Orifice pressure differential corner tappings (Pa)
$\Delta P_{t,fl}$	Orifice pressure differential flange tappings (Pa)
ε	Expansibility factor
γ	Ratio of the vena contracta diameter to pipe diameter
κ	Isentropic exponent
ρ	Density (kg/m^3)
U_p	Average pipe velocity (m/s)
U_p	Average pipe velocity (m/s)

5 REFERENCES

[1] Kocbach J M et al, "Where do we stand on flow metering for CO_2 handling and storage?", 38th International North Sea Flow Measurement Workshop, 26-29 October 2020.

[2] ISO 5167-2, "Measurement of fluid flow by means of pressure differential devices inserted in circular-cross section conduits running full — Part 2: Orifice plates", First edition 2003-03-01.

[3] Morrison G L, DeOtte R E, Nail G H, Panak D L, Texas A & M University, "Mean Velocity and Turbulence Fields Inside a β = 0.50 Orifice Flowmeter", AIChE Journal, May 1993, Vol. 39, No. 5.

[4] Rennels D C and Hudson H M, "Pipe Flow, a Practical and Comprehensive Guide", AIChe 2012.

[5] Reader-Harris M, "Orifice Plates and Venturi Tubes", Experimental Fluid Mechanics, Springer, 2015.

[6] Guide to the Expression of Uncertainty in Measurement, International Organisation for Standardisation, ISO/IEC Guide 98:1995.

[7] Wilson A, Stockton P, Steven R, "Data Reconciliation in Microcosm – Reducing DP Meter Uncertainty", 37th International North Sea Flow Measurement Workshop, 22-25 October 2019.

[8] Wilson A, Stockton P, Steven R, "The Introspective Orifice Meter Uncertainty Improvements", 38th International North Sea Flow Measurement Workshop, 26-29 October 2020.

[9] Buckingham E, "Notes on the orifice meter: the expansion factor for gases", (Research Paper no. 459), 1932.

[10] Urner G, "Technical Note: Pressure loss of orifice plates according to ISO 5167-1", Flow Meas. Instrum., Vol. 8, No. 1, pp. 39–41, 1997.

APPENDIX A SIMPLIFIED MATHEMATICAL MODEL

A.1 Control Volume Upstream to Orifice and Vena Contracta

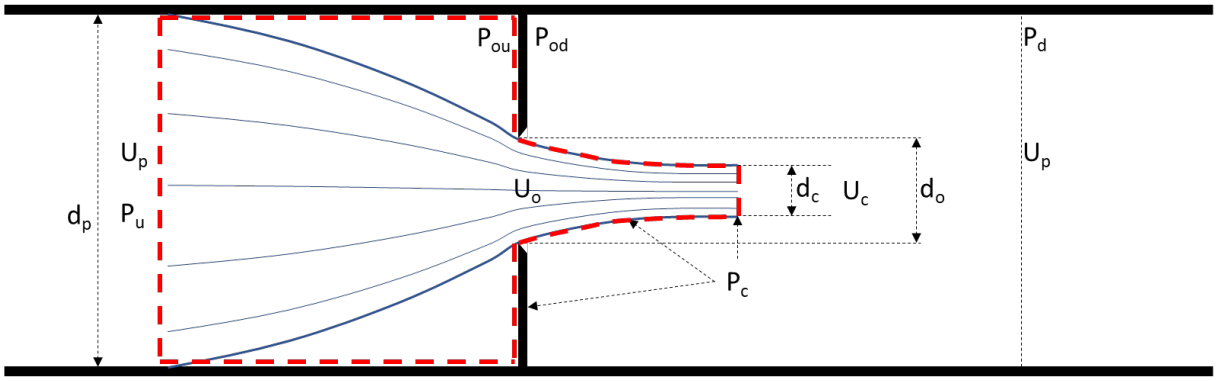

A control volume may be drawn from upstream at P_u just prior to the formation of the orifice jet, along the walls of the pipe and over the upstream face of the orifice plate and continuing over the jet downstream of the orifice terminating at the vena contracta.

Applying mass continuity across the control volume, flow only crosses at two surfaces at the upstream surface and the vena contracta:

$$\rho A_p U_p = \rho A_c U_c \tag{11}$$

Where:

A_c	Area of vena contracta (m^2)
A_p	Area of pipe (m^2)
ρ	Fluid density (kg/m^3)

Simplifying:

$$U_c = U_p \frac{A_p}{A_c} \tag{12}$$

Applying momentum equation across the control surfaces in the horizontal direction:

$$P_u A_p - \left(P_{ou}\left(A_p - A_o\right) + P_c A_o\right) = Q_m U_c - Q_m U_p \tag{13}$$

Where:

A_o	Area of orifice (m^2)
Q_m	Mass flow rate (kg/s)

The forces due to the pressure differential across the vertical surfaces (left and right) of the control volume are equated with the change in momentum of the fluid entering and leaving the control volume across the same control surfaces.

The force due to pressure on the left-hand surface is just the product of P_u and the pipe area. The force due to the pressure on the right-hand surface is P_{ou} upstream of the orifice applied over the whole solid plate area (A_p – A_o) plus P_c applied over the orifice area A_o. It is not just the vena contracta area A_c but also the sides of the cone shaped jet downstream of the orifice in the horizontal direction.

The mass flow rate is given by:

$$Q_m = \rho U_p A_p \tag{14}$$

Substituting for m and dividing through by A_p:

$$P_u - \left(P_{ou}\left(1 - \frac{A_o}{A_p}\right) + P_c \frac{A_o}{A_p}\right) = \rho U_p U_c - \rho U_p^2 \tag{15}$$

Substituting for U_c and expressing area ratios in terms of diameters:

$$P_u - \left(P_{ou}\left(1 - \frac{d_o^2}{d_p^2}\right) + P_c \frac{d_o^2}{d_p^2}\right) = \rho U_p^2 \left(\frac{d_p^2}{d_c^2} - 1\right) \tag{16}$$

Introducing β and γ:

$$P_u - (P_{ou}(1 - \beta^2) + P_c \beta^2) = \rho U_p^2 \left(\frac{1}{\gamma^2} - 1\right) \tag{17}$$

Where:

β Ratio of the orifice diameter to pipe diameter

γ Ratio of the vena contracta diameter to pipe diameter

We can also apply Bernoulli equation across the control volume:

$$P_u + \frac{\rho U_p^2}{2} = P_c + \frac{\rho U_c^2}{2} + L_{uc} \tag{18}$$

Where:

L_{uc} Losses from u to c (Pa)

Rearranging and utilising continuity:

$$P_u - P_c = \frac{\rho U_p^2}{2}\left(\frac{1}{\gamma^4} - 1\right) + L_{uc} \tag{19}$$

A.2 Control Volume from Orifice and Vena Contracta to Downstream

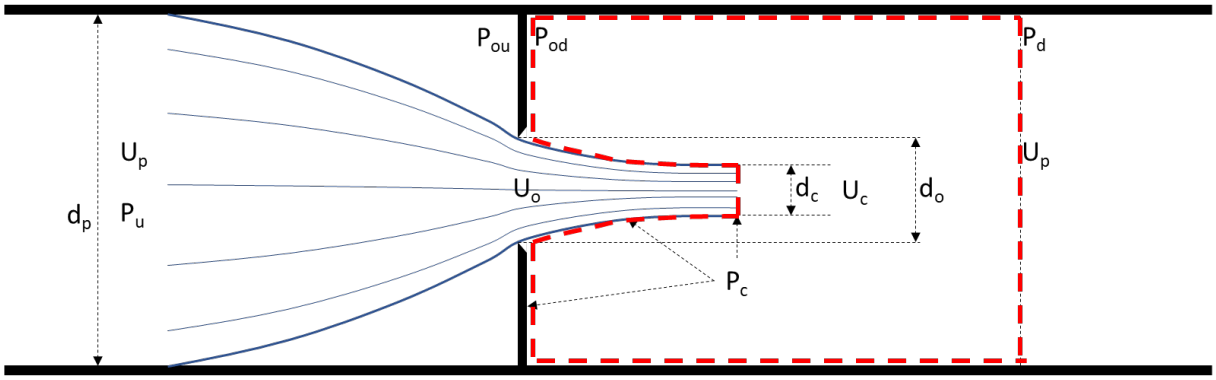

A control volume may be drawn from the back side of the orifice plate and the jet downstream of the orifice terminating at the vena contracta, along the walls of the pipe and over the downstream point of maximum pressure recovery P_d.

The pressure downstream of the orifice at the vena contracta is P_c and assumed to be the same as that just outside the streamlines of the jet and on the back side of

the orifice plate. Hence, P_{od}, the measured pressure at the pipe wall, is assumed to be the same as P_c. Urner [10] applies this same assumption in the development of Equation (7) for the Pressure loss in ISO 5167-2 [2].

Applying momentum equation across the control surfaces in the horizontal direction:

$$P_c A_p - P_d A_p = Q_m U_p - Q_m U_c \tag{20}$$

Substituting for m, U_c and dividing through by A_p:

$$P_d - P_c = \rho U_p^2 \left(\frac{1}{\gamma^2} - 1\right) \tag{21}$$

A.3 Determination of Pipe Velocity (U_p)

We now have three equations (17), (19) and (21) in four unknowns P_u, U_p, γ and L_{uc}. Rearranging them and eliminating P_u and γ, we obtain the following:

$$U_p^2 = \frac{(P_d - P_c)^2}{2\rho\left((1-\beta^2)(P_{ou} - P_c) - L_{uc}\right)} \tag{22}$$

Or in terms of differential pressures:

$$U_p^2 = \frac{\Delta P_r^2}{2\rho\left((1-\beta^2)\Delta P_t - L_{uc}\right)} \tag{23}$$

Where:

ΔP_r Differential pressure recovery ($P_d - P_c$) (Pa)

ΔP_t Differential pressure across orifice ($P_{ou} - P_c$) (Pa)

If the differential pressure across the orifice is replaced by the sum of the recovered and permanent pressure loss:

$$U_p^2 = \frac{\Delta P_r^2}{2\rho\left((1-\beta^2)\left(\Delta P_r + \Delta P_{ppl}\right) - L_{uc}\right)} \tag{24}$$

Where:

ΔP_{ppl} Permanent differential pressure loss ($P_{ou} - P_d$) (Pa)

γ can be calculated by rearranging Equation (21):

$$\gamma = \left(\frac{(P_c - P_d)}{\rho U_p^2} + 1\right)^{-0.5} \tag{25}$$

If the loss term is equated to an equivalent number N_{Luc} of dynamic pressure terms:

$$L_{uc} = \frac{N_{Luc}\rho U_p^2}{2} \tag{26}$$

Substituting in Equation (24) and rearranging to obtain the following expression in U_p:

$$U_p^4 \frac{\rho N_{Luc}}{2} + U_p^2(1-\beta^2)\left(\Delta P_r + \Delta P_{ppl}\right) + \frac{\Delta P_r^2}{2\rho} = 0 \tag{27}$$

Which is a quadratic in U_p^2 and can be determined from:

$$U_p^2 = \frac{(1-\beta^2)\left(\Delta P_r + \Delta P_{ppl}\right) - \sqrt{\left((1-\beta^2)\left(\Delta P_r + \Delta P_{ppl}\right)\right)^2 - N_{Luc}\Delta P_r^2}}{\rho N_{Luc}} \tag{28}$$

A.4 Differential Pressure Conversion from Flange to Corner Tappings

The above analysis is based on differential pressures measured across or with reference to the orifice plate surfaces, i.e., corner tapping measurements. If the measurements are made using flange tappings, then these need to be adjusted to obtain the equivalent pressure differentials for corner tappings.

This performed using the various components of the ISO-5167-2 discharge coefficient C_d which as described in [5], can be broken down into four main terms:

$$C_d = C_\infty + C_s + C_{up} + C_{dn} \tag{29}$$

Where,

C_∞ Discharge coefficient using corner tappings at infinite Reynolds number

C_s Slope term to account for increase in discharge coefficient at lower Reynolds number

C_{up} Tapping term to account for the difference in the discharge coefficient when using an upstream flange tapping compared with a corner tapping

C_{dn} Tapping term to account for the difference in the discharge coefficient when using a downstream flange tapping compared with a corner tapping.

Hence, for corner tappings:

$$Q_m \propto (C_\infty + C_s)\sqrt{\Delta P_t} \tag{30}$$

And, for flange tappings:

$$Q_m \propto \left(C_\infty + C_s + C_{up} + C_{dn}\right)\sqrt{\Delta P_{t,fl}} \tag{31}$$

Where,

$\Delta P_{t,fl}$ Differential pressure measured across flange tappings.

Hence, ΔP_t can be obtained from $\Delta P_{t,fl}$ by:

$$\Delta P_t = \frac{\left(C_\infty + C_s + C_{up} + C_{dn}\right)^2}{(C_\infty + C_s)^2}\Delta P_{t,fl} \tag{32}$$

A similar analysis can be used to convert the recovered and permanent differential pressure measurements based on flanges ($\Delta P_{r,fl}$ and $\Delta P_{ppl,fl}$) to those based on corner tappings:

$$\Delta P_r = \Delta P_{r,fl} + \left(1 - \frac{\left(C_\infty + C_s + C_{up} + C_{dn}\right)^2}{\left(C_\infty + C_s + C_{up}\right)^2}\right)\Delta P_{t,fl} \tag{33}$$

$$\Delta P_{ppl} = \Delta P_{ppl,fl} - \left(1 - \frac{\left(C_\infty + C_s + C_{up} + C_{dn}\right)^2}{(C_\infty + C_s + C_{dn})^2}\right)\Delta P_{t,fl} \tag{34}$$